

Spirocyclic Pyrrolidinyl Nitroxides with Exo-Methylene Substituents

Mateusz P. Sowiński,^[a] Anna-Luisa Warnke,^[a] Bjarte A. Lund,^[a] Susann Skagseth,^[a] David B. Cordes,^[b] Janet E. Lovett,^[c] and Marius M. Haugland^{*[a]}

Nitroxides are stable organic radicals with exceptionally long lifetimes, which render them uniquely suitable as observable probes or polarising agents for spectroscopic investigation of biomolecular structure and dynamics. Radical-based probes for biological applications are ideally characterized by both robustness towards reductive degradation and beneficial electron spin relaxation parameters. These properties are largely influenced by the molecular structure of the nitroxide scaffold, and also by the conformations it prefers to adopt. In this study we present the synthesis of the first nitroxides based on a spirocyclic pyrrolidine scaffold with an exocyclic methylene substituent.

The conformations adopted by these nitroxides were evaluated by X-ray crystallography, both with single nitroxide crystals and by inclusion of nitroxides in a microporous crystalline sponge. The kinetic and thermodynamic stability of the new nitroxides towards reduction was investigated by electron paramagnetic resonance (EPR) spectroscopy and cyclic voltammetry (CV). In combination with EPR measurements of electron spin relaxation properties, these results suggest that this new family of nitroxides can provide access to multifunctionalized probes and polarising agents suitable for use in biological environments at elevated temperatures.

Introduction

Nitroxides (aminoxyl radicals) are a class of stable organic radicals where the unpaired electron is stabilized by steric shielding and delocalisation over the N–O bond.^[1] The extremely long lifetimes of nitroxide radicals render them suitable for various applications in spectroscopy, in particular for investigations in structural biology. Nitroxides have gained a unique place within electron paramagnetic resonance (EPR) spectroscopy as spin labels that can reveal dynamic and structural information in biomolecules.^[2] Through a process known as site-directed spin labelling (SDSL), nitroxides can be covalently attached to the biomolecule of interest, which is then analysed by EPR spectroscopy.^[3] This approach is especially powerful when integrated with the double electron-electron resonance (DEER) experiment (also known as pulsed electron-electron double resonance, PELDOR), which can extract the interspin distance and relative orientation of two paramagnetic centres within a biomolecule or biomolecular

complex.^[2a,4] Nitroxides also hold a firmly established position as polarising agents for sensitivity enhancement by dynamic nuclear polarisation (DNP) in nuclear magnetic resonance (NMR) spectroscopy, a technique that is of particular utility in the study of large biomolecules.^[5] This ability to transfer spin polarisation to the surrounding medium has, moreover, led to the development of nitroxides as promising metal-free contrast agents for MRI imaging.^[6]

In order to be suitable for these numerous applications in spectroscopy and imaging, nitroxide derivatives should ideally exhibit robustness towards reduction, possess optimal electron spin relaxation times, and be adequately soluble in aqueous environments.^[2b] The need for stability towards reduction arises from a tendency for nitroxides to be converted to diamagnetic hydroxylamines in reducing media, such as the intracellular environment. Numerous reducing agents have been implied in this process, including ascorbic acid, glutathione, free thiols and enzymes.^[7] Several factors determine the reductive stability of nitroxides, including the presence of charges, electron-donating or -withdrawing functional groups, the size of the nitroxide ring, and the steric bulkiness of the substituents at the quaternary α -positions next to the paramagnetic centre (Figure 1).^[8] Saturated five-membered pyrrolidinyl nitroxides are remarkably stable when compared to unsaturated five-membered pyrrolinyl and the least stable six-membered piperidinyl nitroxides (Figure 1a, top).^[8d,9] Tetraethyl substituents surrounding the nitroxide impart increased steric shielding, thereby contributing to exceptional stability compared to their tetramethyl counterparts (Figure 1a, bottom).^[8c] Spirocyclohexyl moieties, meanwhile, offer some improvement in stability over tetramethyl substituents,^[8c] but their most significant advantage lies in the excellent electron spin relaxation parameters exhibited by spirocyclic nitroxides (Figure 1b).^[10] The parameter that is most important to the resolution and range of distance

[a] M. P. Sowiński, A.-L. Warnke, B. A. Lund, S. Skagseth, M. M. Haugland
Department of Chemistry, UiT The Arctic University of Norway, Tromsø
9037, Norway
E-mail: marius.m.haugland@uit.no

[b] D. B. Cordes
EaStCHEM School of Chemistry, University of St Andrews, North Haugh, St
Andrews KY16 9ST, UK

[c] J. E. Lovett
SUPA School of Physics and Astronomy and BSRC, University of St Andrews,
North Haugh, St Andrews KY16 9SS, UK

Supporting information for this article is available on the WWW under
<https://doi.org/10.1002/cplu.202400387>

© 2024 The Authors. ChemPlusChem published by Wiley-VCH GmbH. This is
an open access article under the terms of the Creative Commons Attribution
License, which permits use, distribution and reproduction in any medium,
provided the original work is properly cited.

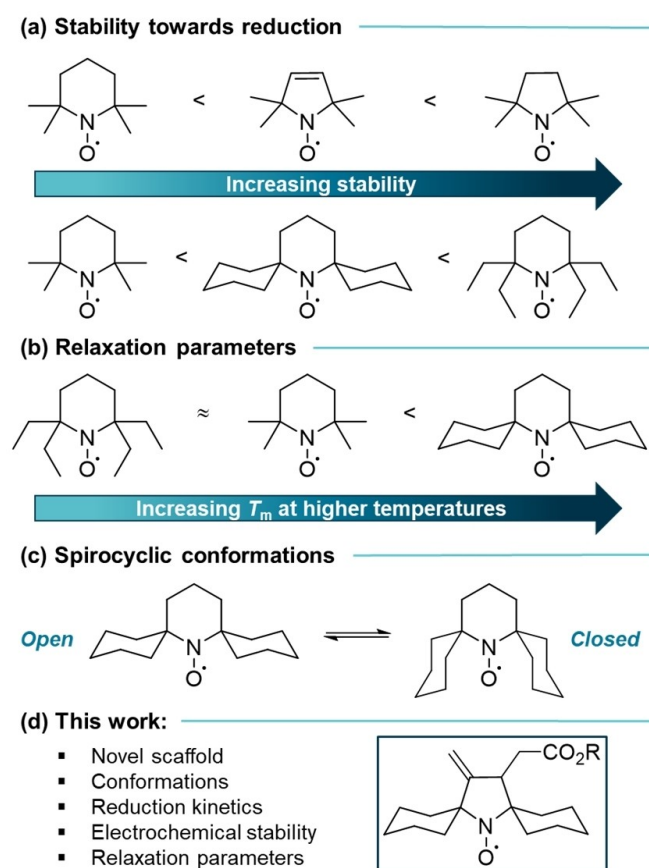


Figure 1. Trends in nitroxide stability and relaxation properties. a) Effects of ring size and quaternary substituents on stability. b) Influence of α -substituents on relaxation times T_m . c) This work.

measurements in the DEER experiment, known as the phase memory time (T_m), is related to transverse relaxation of the electron spin. T_m is negatively impacted by the rotation of methyl groups,^[11] a process that becomes particularly pronounced at temperatures above 70 K, due to coupling between the electron spin and the ^1H nuclear spin.^[12] Despite several efforts to develop nitroxide probes that display extended relaxation times at elevated temperatures,^[13] the combined requirement for low temperatures and reduction-resistant nitroxides limits the potential of EPR and other electron spin-based technologies in biological systems under physiological conditions.

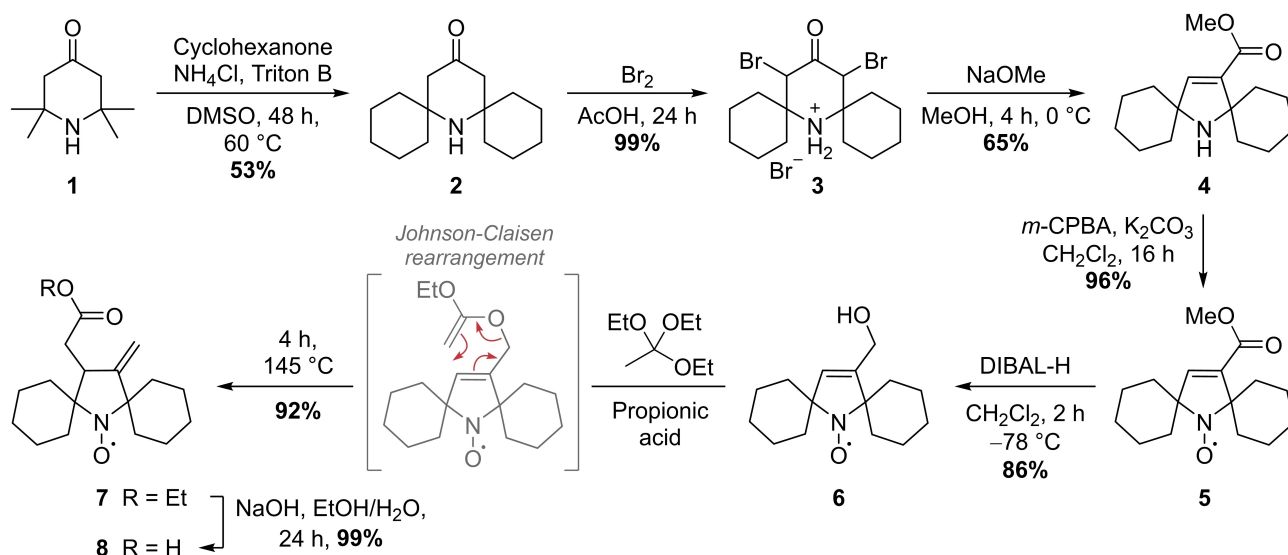
In previous work we demonstrated that implementing additional substituents in piperidiny nitroxides can induce spirocyclic scaffolds to adopt *closed* conformations (Figure 1c).^[14] In these conformations the spirocyclic groups provide more efficient steric shielding of the nitroxide radical centre, which leads to enhanced stability towards reduction while simultaneously maintaining the excellent relaxation properties of spirocyclic nitroxide scaffolds. However, as the 5-membered pyrrolidiny and pyrrolidiny nitroxides are inherently even more stable, we hypothesized that the introduction of additional substituents in these scaffolds could result in nitroxides adopting *closed* conformations with even higher stabilities. In

this study, we report the development of a novel family of spirocyclic pyrrolidiny nitroxides with an exocyclic methylene substituent (Figure 1d). The conformations adopted by nitroxides based on this scaffold were investigated by single crystal X-ray diffraction (SC-XRD), and stability to reduction was assessed by continuous wave (CW) EPR spectroscopy and cyclic voltammetry (CV). The electron spin relaxation parameters T_m and T_1 of nitroxides based on this new scaffold were also measured by pulsed EPR methods across a range of temperatures. Our findings indicate that the new spirocyclic exomethylene nitroxides are promising scaffolds for the development of reduction resistant spin labels for elevated-temperature DEER measurements or DNP polarising agents.

Results and Discussion

We hypothesized that an exocyclic methylene group could induce spirocyclic pyrrolidiny nitroxides to adopt *closed* conformations, in analogy to our previous work. To access this scaffold, we devised a synthetic route relying on a Johnson-Claisen rearrangement (Scheme 1). A similar strategy has previously been demonstrated with less sterically congested tetramethyl-substituted nitroxides.^[15] The synthesis began with commercially available 2,2,6,6-tetramethyl-4-piperidone **1**, which can be transformed into the spirocyclic equivalent **2** via a previously described ketone exchange method.^[16] Ring contraction was accomplished through dibromination of ketone **2** and subsequent treatment of the dibrominated hydrobromide salt **3** with freshly prepared sodium methoxide, resulting in a Favorskii rearrangement to pyrroline methyl ester **4**.^[17] Amine oxidation with *meta*-chloroperbenzoic acid (*m*-CPBA) led to the formation of nitroxide **5**, and the ester was reduced to the allylic alcohol **6** using diisobutylaluminium hydride (DIBAL-H). This key intermediate was heated in the presence of triethyl orthoacetate and catalytic acid, resulting in a thermal Johnson-Claisen rearrangement to the *exo*-methylene substituted pyrrolidine nitroxide ethyl ester **7** in excellent yield.

With the scaffold of interest in hand, our attention turned towards investigating the conformations adopted by the spirocyclohexyl moieties. The direct application of two-dimensional NMR spectroscopy to investigate the conformations of nitroxides is prevented by severe signal broadening caused by paramagnetic relaxation enhancement. Although *in situ* reduction of the nitroxide to a diamagnetic hydroxylamine can enable investigation of these scaffolds by NMR, significant overlap of the resonances of the diagnostic spirocyclic protons makes this approach highly challenging. As reduction to a hydroxylamine leads to a pyramidalization of the otherwise planar nitroxide, this approach can, moreover, alter the conformational distribution of the nitroxides. Instead, we opted for single-crystal X-ray diffraction (SC-XRD) as the optimal method to assess nitroxide conformations. Among the five-membered nitroxides with known X-ray structures, a majority adopt either *open* or *semi-open* conformations.^[18] Although nitroxide **7** is an oil in neat form, we were able to prepare a metal-organic framework (MOF) inclusion complex of this



Scheme 1. Synthetic route towards *exo*-methylene substituted spirocyclic pyrrolidinylnitroxides.

nitroxide and successfully determine its crystal structure by the crystalline sponge method (Figure 2a).^[19] This structure clearly shows that nitroxide **7** adopts an *open* conformation (Figure 2b). We were also able to hydrolyse ester **7** to the carboxylic acid **8** (Scheme 1), which amusingly is a crystalline solid. The solid-state structure of nitroxide **8** was also determined through X-ray crystallography, revealing that the spirocyclohexyl substituents adopt an *open* conformation in the solid state even outside the microporous MOF environment (Figure 2c). Although these results suggest that the *exo*-methylene substituent does not bias nitroxides toward adopting *closed* conformations, our prior research on substituted nitroxides has revealed that the solid-state structure does not always accurately reflect the behaviour observed in solution.^[14] Therefore, it was nevertheless of significant interest to explore the

kinetic and thermodynamic stability of *exo*-methylene nitroxides towards redox reactions.

We next recorded kinetic decay curves of nitroxides (2 mM in a PBS buffer/DMSO solution 1:1 *v/v*) in the presence of sodium ascorbate (16 equivalents) as a simple model of a reducing environment. Nitroxide reduction was monitored by CW-EPR spectroscopy at X-band frequencies by observing the decreasing peak intensity of the characteristic triplet spectrum over time (Figure 3). At these relatively high concentrations the measurements exhibited a rapid decay within the initial seconds. Such apparent deviation from pseudo-first-order behaviour is consistent with the complex mechanism of ascorbate degradation, especially under aerobic conditions.^[7a,8e] Consequently, determining the absolute rate constants is not possible. Nevertheless, a comparison of the reduction profiles remains a valid indication of the relative kinetic stability of

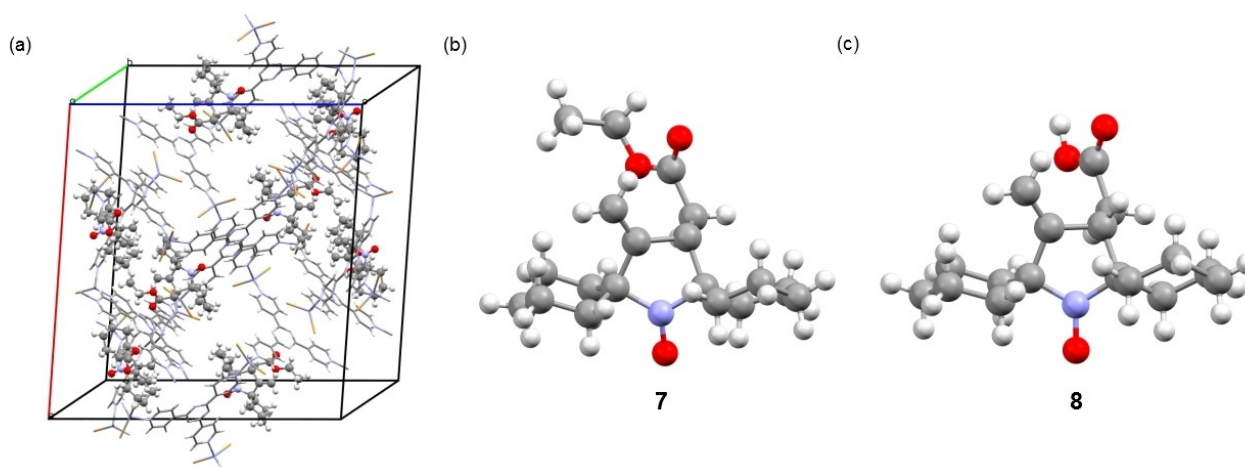


Figure 2. X-ray crystal structures of *exo*-methylene substituted nitroxides. a) Structure of nitroxide **7** embedded within the MOF lattice $\{[(ZnBr_2)_3(\text{tris}(4\text{-pyridyl})\text{-}1,3,5\text{-triazine})_2]_x(\text{CHCl}_3)_y\}_n$. Solvent molecules are removed for clarity. b) Structure of nitroxide **7**. The MOF lattice is removed. c) Structure of nitroxide **8**.

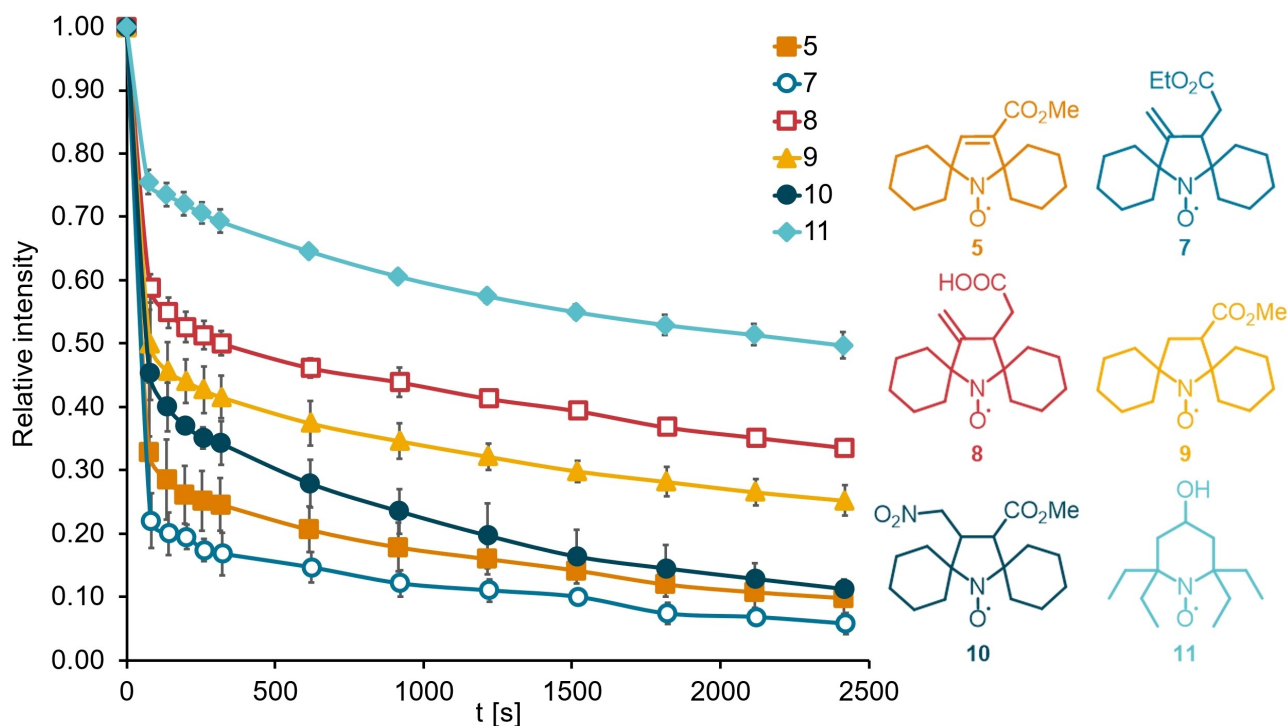


Figure 3. Pseudo-first-order kinetic reduction curves of nitroxides (2 mM) with sodium ascorbate (16 equiv.) in PBS buffer/DMSO (1:1) at 293 K. Data points are the average of three runs, with error bars representing $2 \times$ standard deviation.

these nitroxides. The stability of *exo*-methylene-substituted nitroxides **7** and **8** was benchmarked against the established monosubstituted pyrrolinyl and pyrrolidinyl nitroxides **5** and **9**, respectively (Figure 3). Additionally, **7** and **8** were compared with the disubstituted pyrrolidinyl nitroxide **10** (as a mixture of diastereomers) and the most stable species from our previous research, tetraethyl-substituted piperidinyl nitroxide **11** (see the Supporting Information for synthesis).^[14]

The tetraethyl-substituted piperidinyl nitroxide **11** remains the most stable also in this set of nitroxides, exhibiting 50% remaining radical after exposure to an excess of reducing agent for 40 minutes. By comparison, all the spirocyclohexyl-substituted nitroxides were more rapidly reduced, presumably due to the less effective steric shielding provided by the spirocyclohexyl moieties. The difference in stability between pyrrolinyl nitroxide **5** (10% remaining radical) and pyrrolidinyl nitroxide **9** (25% remaining radical) is evident. This finding is in contrast with previous studies that indicate a negligible difference in reduction stability between spirocyclohexyl-substituted pyrrolinyl and pyrrolidinyl nitroxides, which has been ascribed to subtle differences in the relative population of *open* and *semi-open* conformations in these scaffolds.^[18a] Pyrrolidinyl nitroxides, which are inherently more stable towards reduction, prefer *open* scaffold conformations that leave the radical centre more exposed and thereby facilitate reaction with ascorbate. By contrast, pyrrolinyl nitroxides favour *semi-open* conformations that partially shield the nitroxide group, thereby compensating for the effect of the intrinsically less stable unsaturated ring.^[18a] These apparently contradictory results can, however, be explained by differences in the conditions and the functional

groups present in the nitroxides between this previous study and our work, both of which can have a significant impact on kinetic rates.^[18a] Interestingly, the novel disubstituted pyrrolidinyl nitroxide **10** (11% remaining radical) has a comparable stability to pyrrolinyl nitroxide **5**. Here, it is possible that the stability expected for a pyrrolidinyl nitroxide (e.g. **9**) is counterbalanced by the electronic effects of the nitro functionality.

The novel *exo*-methylene pyrrolidinyl nitroxide **7**, meanwhile, exhibits slightly faster reduction kinetics than the benchmark pyrrolinyl nitroxide **5** (6% remaining radical). This suggests that any difference in inherent stability of the *exo*-methylene pyrrolidinyl nitroxide scaffold compared to the pyrrolinyl scaffold can be compensated by a conformational shift of the opposite effect. Compared to ester **7**, however, the carboxylic acid **8** exhibits the greatest stability among the examined spirocyclic nitroxides (34% remaining radical). Under the experimental conditions this compound is present in the anionic carboxylate form, which is known to provide stabilization through inductive electronic and electrostatic effects.^[8e,18a] These effects clearly have a much larger impact on reduction rates than the saturation and substitution pattern of the nitroxide core ring.

To evaluate the thermodynamic stability profiles of the new nitroxide scaffolds, we next assessed their redox behaviour by cyclic voltammetry (Figure 4). Voltammograms of the nitroxides **5**, **7** and **8** (20 μ mol) in a 0.1 M solution of tetrabutylammonium hexafluorophosphate (TBAPF₆) in acetonitrile were recorded using a three-electrode setup, with a 3 mm diameter glassy carbon electrode as the working electrode, platinum wire as the counter electrode and a saturated calomel electrode (SCE) as

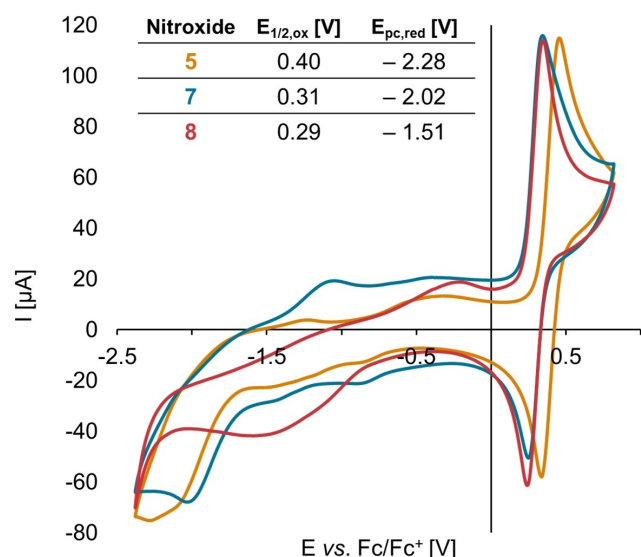


Figure 4. Cyclic voltammograms (CVs) of the nitroxides **5**, **7** and **8** (20 μmol) in 0.1 M solution of TBAPF_6 in acetonitrile (10 mL). CVs are plotted according to the IUPAC convention. Measurements were performed with 100 mV/s scan rate, in the anodic direction. Oxidation potentials were determined. Reduction potentials were estimated as cathodic peak potential due to irreversible behaviour.

the reference electrode (potentials were referenced to the ferrocene/ferrocenium redox pair) with 100 mV/s scan rate. Peak couples in the anodic region correspond to the reversible oxidation of the nitroxides to the corresponding oxoammonium cations. *Exo*-methylene nitroxides **7** and **8** exhibit lower oxidation potentials than the reference pyrrolinyl nitroxide **5**, presumably due to the additional methylene carbon and absence of conjugation between the electron-withdrawing ester/acid functionality and the core nitroxide ring.^[8a] The cathodic peaks arise from reduction of the nitroxides to hydroxylamines through a single-electron reduction (via aminoxylate anions) coupled with proton transfer. This process is quasi-reversible or irreversible under the conditions of the measurement, meaning the reduction potentials could only be estimated. It is known that the presence of functional groups that typically stabilize the reduced form result in a decrease in the reduction potential (i.e. less negative values).^[20] Surprisingly, however, the reduction potential of *exo*-methylene nitroxide **7** (−2.02 V) is lower than the reduction potential for pyrrolinyl nitroxide **5** (−2.28 V), despite the additional methylene unit between the electron-withdrawing functional group and the core nitroxide ring. Thus, the redox window for the new *exo*-methylene pyrrolidinyl nitroxides is narrower than for pyrrolinyl nitroxides. The reduction potential of acid **8** is even lower (−1.51 V). We hypothesize that this anomaly can be explained by stabilization of the reduced (aminoxylate) form of nitroxide **8** by intramolecular hydrogen bonding with the carboxylic acid functionality. A similar effect has been observed in piperidinyl nitroxides.^[21]

Beyond stability towards reduction, relaxation behaviour is a crucial consideration for the use of nitroxides for measure-

ments and imaging in biological systems. We therefore next investigated the relaxation parameters T_m and T_1 for the new *exo*-methylene pyrrolidine nitroxide **8**. The phase memory time T_m is a measure of the decay rate of an electron spin Hahn echo, which is an important factor for the resolution and range of pulsed EPR experiments such as DEER. Spin echo decay curves were measured across a range of temperatures (Figure 5a), and from these the phase memory time T_m was extracted. T_m remains relatively stable at temperatures up to 160 K ($T_{m,50\text{K}}=4.15\ \mu\text{s}$ and $T_{m,160\text{K}}=3.29\ \mu\text{s}$, which corresponds to 79% of $T_{m,50\text{K}}$). However, a significant change occurs at 180 K ($T_{m,180\text{K}}=0.85\ \mu\text{s}$), which may be due to increased dynamic motion as the water/glycerol glass softens. The change in spin echo dephasing rates (i.e. the reciprocal of T_m) across different temperatures for nitroxide **8** (Figure 5b) can also be compared with the reference nitroxides TEMPOL (**12**), TEEPOL (**11**), and 4-hydroxyspirocyclohexylpiperidine 1-oxyl (**13**). The advantages of nitroxides with spirocyclic α -substituents in terms of relaxation parameters are clearly illustrated, as the absence of the relaxation mechanism provided by rotatable methyl groups extends the useful temperature range of such nitroxides well above the usual cutoff of 50–70 K for **11** and **12**.^[12]

The longitudinal relaxation time T_1 of the electron spin is a measure of the transfer of polarisation from the paramagnetic centre to the surrounding lattice. This process is crucial in techniques such as magic angle spinning dynamic nuclear polarisation (MAS-DNP) in solid-state NMR spectroscopy,^[5a]

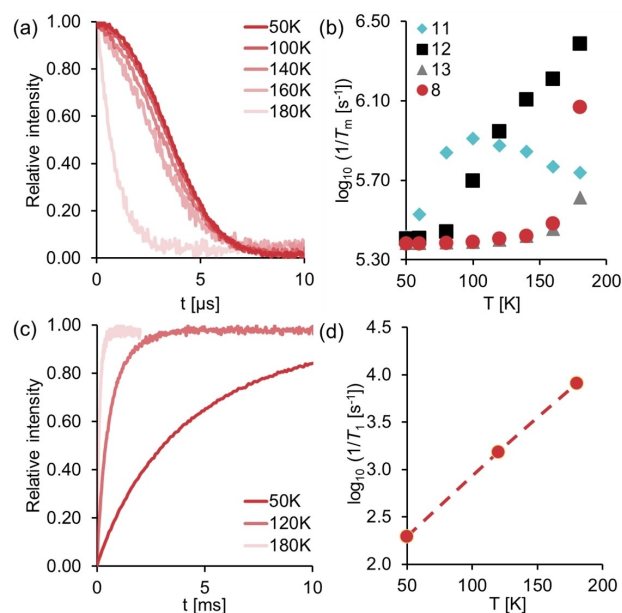


Figure 5. Relaxation parameters of the nitroxide **8** (50 μM solution in glycerol/PBS buffer/DMSO 1000:999:1 v/v) measured by Q-band EPR spectroscopy. a) Spin echo decay curves for the nitroxide **8** at various temperatures. b) Logarithm of the reciprocal of T_m vs temperature for **8** and other reference nitroxides, measured by spin echo decay. c) Inversion recovery of the longitudinal relaxation time T_1 for the nitroxide **8** at various temperatures. Data at 50 K is truncated in the figure only; T_1 is determined on the complete measurement data (shown in Figure S11 of the Supporting Information). d) Logarithm of the reciprocal of T_1 vs temperature for the nitroxide **8**, measured by inversion recovery.

where long T_1 times can lead to loss of signal intensity by depolarisation.^[22] T_1 is also an important consideration in the development of MRI contrast agents.^[6a] The spin-lattice relaxation of nitroxide **8** was measured by inversion recovery at different temperatures (Figure 5c), from which numerical values for T_1 were found to be 5.2 ms (50 K), 0.65 ms (120 K), and 0.12 ms (180 K). The logarithm of the spin-lattice relaxation rate (i.e. $\log_{10}(T_1^{-1})$) appears to show the expected linear dependence on temperature (Figure 5d).^[23]

Conclusions

In conclusion, we have developed a synthetic route to new spirocyclic nitroxide pyrrolidine scaffolds with an exocyclic methylene substituent. Surprisingly, this additional substituent does not appear to significantly influence the conformations adopted by the scaffold, as indicated by X-ray crystallography. Kinetic decay measurements with EPR monitoring show that the presence of the *exo*-methylene substituent does not lead to increased stability of the nitroxide under reducing conditions. A carboxylate functionality, however, is found to have a considerable stabilizing effect, even when located at a remote position in the scaffold. Circular voltammetry measurements indicate that the thermodynamic redox window of nitroxides based on the new *exo*-methylene scaffold is slightly narrower than nitroxides from the more established pyrroline family. The electron spin relaxation properties of the new nitroxides, meanwhile, are unaffected by the additional *exo*-methylene group, with excellent phase coherence times (T_m) maintained until 160 K as measured by pulsed EPR methods.

Although the new substituted spirocyclic nitroxides reported in this work do not exhibit improved stability, we note that the *exo*-methylene unit can serve as a useful synthetic handle for further elaboration.^[15,24] We therefore believe that these scaffolds will be useful intermediates, e.g. in the synthesis of multifunctionalized nitroxide-based spin labels or polarising agents.

Supporting Information Summary

Supporting Information available. General procedures and materials, synthesis and characterization of nitroxides and intermediates, crystallography procedures, as well as key crystal properties (Table S1) are given. Moreover, copies of CW EPR spectra of measured nitroxides (Figures S1–S8), kinetic decay curves (Figure S9), relaxation measurements (Figures S10–S11) and copies of NMR spectra (Figures S12–S44) are included. The authors have cited additional references within the Supporting Information.^[25–33]

Acknowledgements

M.P.S., A.-L.W. and M.M.H. thank the Tromsø Research Foundation and UiT Centre for New Antibacterial Strategies (CANS) for

a start-up grant (TFS project ID: 18_CANS). J.E.L. thanks Drs Hassane El Mkami and Robert I. Hunter for technical assistance, the BBSRC (BB/T017740/1) and the Wellcome Trust (099149/Z/12/Z) for the Q-band EPR spectrometer, and the Royal Society for Research Grant RG120645 for the benchtop spectrometer.

Conflict of Interests

The authors declare no conflict of interest.

Data Availability Statement

A previous version of this work prior to peer review has been posted on a preprint server.^[34] Deposition Numbers 2356140 (for MOF-embedded **7**) and 2348068 (for **8**) contain the supplementary crystallographic data for this paper. These data are provided free of charge by the joint Cambridge Crystallographic Data Centre and Fachinformationszentrum Karlsruhe Access Structures service. Additional raw data is available through the DataverseNO repository at <https://doi.org/10.18710/PIZ7H1>.^[35]

Keywords: EPR spectroscopy · Nitroxide · Radicals · Relaxation · Stability

- [1] H. Karoui, F. L. Moigne, O. Ouari, P. Tordo, in *Stable Radicals* (Ed: R. G. Hicks), John Wiley & Sons, Ltd 2010, 173–229.
- [2] a) M. M. Haugland, E. A. Anderson, J. E. Lovett, in *Electron Paramagnetic Resonance* (Eds: V. Chechik, D. M. Murphy), Vol. 25, Royal Society of Chemistry 2016, 1–34; b) M. M. Haugland, J. E. Lovett, E. A. Anderson, *Chem. Soc. Rev.* 2018, 47, 668–680.
- [3] S. A. Shelke, S. T. Sigurdsson, in *Structural Information from Spin-Labels and Intrinsic Paramagnetic Centres in the Biosciences*, Vol. 152, Springer, Berlin 2011, 121–162.
- [4] a) J. F. W. Keana, *Chem. Rev.* 1978, 78, 37–64; b) V. V. Khramtsov, in *Nitroxides* (Eds: O. Ouari, D. Gimes), The Royal Society of Chemistry 2021, 147–186; c) H. El Mkami, D. G. Norman, *Methods Enzymol.* 2015, 564, 125–152.
- [5] a) T. Biedenbänder, V. Aladin, S. Saeidpour, B. Corzilius, *Chem. Rev.* 2022, 122, 9738–9794; b) G. Menzildjian, J. Schlagnitweit, G. Casano, O. Ouari, D. Gajan, A. Lesage, *Chem. Sci.* 2023, 14, 6120–6148; c) D. J. Kubicki, G. Casano, M. Schwarzwälder, S. Abel, C. Sauvée, K. Ganesan, M. Yulikov, A. J. Rossini, G. Jeschke, C. Copéret, A. Lesage, P. Tordo, O. Ouari, L. Emsley, *Chem. Sci.* 2016, 7, 550–558.
- [6] a) A. Rajca, Y. Wang, M. Boska, J. T. Paletta, A. Olanikitwanit, M. A. Swanson, D. G. Mitchell, S. S. Eaton, G. R. Eaton, S. Rajca, *J. Am. Chem. Soc.* 2012, 134, 15724–15727; b) H. V.-T. Nguyen, Q. Chen, J. T. Paletta, P. Harvey, Y. Jiang, H. Zhang, M. D. Boska, M. F. Ottaviani, A. Jasanoff, A. Rajca, J. A. Johnson, *ACS Cent. Sci.* 2017, 3, 800–811; c) O. U. Akakuru, M. Z. Iqbal, M. Saeed, C. Liu, T. Paunesku, G. Woloschak, N. S. Hosmane, A. Wu, *Bioconjugate Chem.* 2019, 30, 2264–2286.
- [7] a) A. A. Bobko, I. A. Kirilyuk, I. A. Grigor'ev, J. L. Zweier, V. V. Khramtsov, *Free Radical Biol. Med.* 2007, 42, 404–412; b) M. Azarkh, O. Okle, P. Eyring, D. R. Dietrich, M. Drescher, *J. Magn. Reson.* 2011, 212, 450–454; c) K. M. McCoy, R. Rogawski, O. Stovicek, A. E. McDermott, *J. Magn. Reson.* 2019, 303, 115–120; d) A. Rančić, N. Babić, M. Orio, F. Peyrot, *Antioxidants* 2023, 12, 402; e) M. S. Usatov, S. A. Dobrynin, Y. F. Polienko, D. A. Morozov, Y. I. Glazachev, S. V. An'kov, T. G. Tolstikova, Y. V. Gatilov, I. Y. Bagryanskaya, A. E. Raizvikh, E. G. Bagryanskaya, I. A. Kirilyuk, *Int. J. Mol. Sci.* 2024, 25, 1550.
- [8] a) S. Morris, G. Sosnovsky, B. Hui, C. O. Huber, N. U. M. Rao, H. M. Swartz, *J. Pharm. Sci.* 1991, 80, 149–152; b) S. Okazaki, M. Abdul Mannan, K. Sawai, T. Masumizu, Y. Miura, K. Takeshita, *Free Radical Res.* 2007, 41,

- 1069–1077; c) T. Yamasaki, F. Mito, Y. Ito, S. Pandian, Y. Kinoshita, K. Nakano, R. Murugesan, K. Sakai, H. Utsumi, K.-I. Yamada, *J. Org. Chem.* **2011**, *76*, 435–440; d) J. T. Paletta, M. Pink, B. Foley, S. Rajca, A. Rajca, *Org. Lett.* **2012**, *14*, 5322–5325; e) A. P. Jagtap, I. Krstic, N. C. Kunjir, R. Hänsel, T. F. Prisner, S. T. Sigurdsson, *Free Radical Res.* **2015**, *49*, 78–85; f) I. F. Zhurko, S. A. Dobrynin, Y. I. Glazachev, Y. V. Gatilov, I. A. Kirilyuk, *Molecules* **2024**, *29*, 599.
- [9] Y. Wang, J. T. Paletta, K. Berg, E. Reinhart, S. Rajca, A. Rajca, *Org. Lett.* **2014**, *16*, 5298–5300.
- [10] E. V. Zaytseva, D. G. Mazhukin, *Molecules* **2021**, *26*, 677.
- [11] A. Rajca, V. Kathirvelu, S. K. Roy, M. Pink, S. Rajca, S. Sarkar, S. S. Eaton, G. R. Eaton, *Chem. Eur. J.* **2010**, *16*, 5778–5782.
- [12] K. Nakagawa, M. B. Candelaria, W. W. C. Chik, S. S. Eaton, G. R. Eaton, *J. Magn. Reson.* **1992**, *98*, 81–91.
- [13] a) Z. Yang, R. A. Stein, T. Ngendahimana, M. Pink, S. Rajca, G. Jeschke, S. S. Eaton, G. R. Eaton, H. S. Mchaourab, A. Rajca, *J. Phys. Chem. B* **2020**, *124*, 3291–3299; b) Z. Yang, R. A. Stein, M. Pink, P. Madzellan, T. Ngendahimana, S. Rajca, M. A. Wilson, S. S. Eaton, G. R. Eaton, H. S. Mchaourab, A. Rajca, *J. Am. Chem. Soc.* **2023**, *145*, 25726–25736.
- [14] M. P. Sowiński, S. Gahlawat, B. A. Lund, A.-L. Warnke, K. H. Hopmann, J. E. Lovett, M. M. Haugland, *Commun. Chem.* **2023**, *6*, 111.
- [15] K. Hideg, C. P. Sár, O. H. Hankovszky, T. Tamás, G. Jerkovich, *Synthesis* **1993**, 390–394.
- [16] K. Sakai, K.-I. Yamada, T. Yamasaki, Y. Kinoshita, F. Mito, H. Utsumi, *Tetrahedron* **2010**, *66*, 2311–2315.
- [17] a) G. Sosnovsky, Z.-W. Cai, *J. Org. Chem.* **1995**, *60*, 3414–3418; b) A. Babič, S. Pečar, *Synlett* **2008**, 1155–1158.
- [18] a) I. A. Kirilyuk, Y. F. Polienko, O. A. Krumkacheva, R. K. Strizhakov, Y. V. Gatilov, I. A. Grigor'ev, E. G. Bagryanskaya, *J. Org. Chem.* **2012**, *77*, 8016–8027; b) Y. F. Polienko, N. M. Kuprikova, D. A. Parkhomenko, Y. V. Gatilov, E. I. Chernyak, I. A. Kirilyuk, *Tetrahedron* **2021**, *81*, 131915; c) D. A. Morozov, I. A. Kirilyuk, D. A. Komarov, A. Goti, I. Y. Bagryanskaya, N. V. Kuratieva, I. A. Grigor'ev, *J. Org. Chem.* **2012**, *77*, 10688–10698; d) Y. V. Khoroshunova, D. A. Morozov, D. A. Kuznetsov, T. V. Rybalova, Y. I. Glazachev, E. G. Bagryanskaya, I. A. Kirilyuk, *Int. J. Mol. Sci.* **2023**, *24*, 11498.
- [19] a) T. R. Ramadhar, S.-L. Zheng, Y.-S. Chen, J. Clardy, *Chem. Commun.* **2015**, *51*, 11252–11255; b) T. R. Ramadhar, S.-L. Zheng, Y.-S. Chen, J. Clardy, *Acta Crystallogr. Sect. A Found. Adv.* **2015**, *71*, 46–58; c) A. D. Cardenal, T. R. Ramadhar, *ACS Cent. Sci.* **2021**, *7*, 406–414; d) Y. Inokuma, S. Yoshioka, J. Ariyoshi, T. Arai, Y. Hitora, K. Takada, S. Matsunaga, K. Rissanen, M. Fujita, *Nature* **2013**, *495*, 461–466.
- [20] S. Manda, I. Nakanishi, K. Ohkubo, H. Yakumaru, K.-I. Matsumoto, T. Ozawa, N. Ikota, S. Fukuzumi, K. Anzai, *Org. Biomol. Chem.* **2007**, *5*, 3951–3955.
- [21] J. P. Blinco, J. L. Hodgson, B. J. Morrow, J. R. Walker, G. D. Will, M. L. Coote, S. E. Bottle, *J. Org. Chem.* **2008**, *73*, 6763–6771.
- [22] F. Mentink-Vigier, S. Paul, D. Lee, A. Feintuch, S. Hediger, S. Vega, G. De Paëpe, *Phys. Chem. Chem. Phys.* **2015**, *17*, 21824–21836.
- [23] H. Sato, S. E. Bottle, J. P. Blinco, A. S. Micallef, G. R. Eaton, S. S. Eaton, *J. Magn. Reson.* **2008**, *191*, 66–77.
- [24] T. Kálai, B. Rozsnyai, G. Jerkovich, K. Hideg, *Synthesis* **1994**, 1079–1082.
- [25] Apex3, Bruker AXS Inc., Madison (WI), USA **2018**.
- [26] *CrysAlisPro* v1.171.42.83a. Rigaku Oxford Diffraction, Rigaku Corporation, Oxford, U. K. **2023**.
- [27] G. M. Sheldrick, *Acta Crystallogr. Sect. A Found. Adv.* **2015**, *71*, 3–8.
- [28] G. M. Sheldrick, *Acta Crystallogr. Sect. C Struct. Chem.* **2015**, *71*, 3–8.
- [29] A. L. Spek, *Acta Crystallogr. Sect. D* **2009**, *65*, 148–155.
- [30] A. L. Spek, *Acta Crystallogr. Sect. C Struct. Chem.* **2015**, *71*, 9–18.
- [31] O. V. Dolomanov, L. J. Bourhis, R. J. Gildea, J. A. K. Howard, H. Puschmann, *J. Appl. Crystallogr.* **2009**, *42*, 339–341.
- [32] K. Hideg, H. O. Hankovszky, H. A. Halász, P. Sohár, *J. Chem. Soc.-Perkin Trans.* **1988**, *1*, 2905–2911.
- [33] C. Wetter, J. Gierlich, C. A. Knoop, C. Müller, T. Schulte, A. Studer, *Chem. Eur. J.* **2004**, *10*, 1156–1166.
- [34] M. P. Sowiński, A.-L. Warnke, B. A. Lund, S. Skagseth, D. B. Cordes, J. E. Lovett, M. M. Haugland, *ChemRxiv preprint* **2024**, DOI: 10.26434/chemrxiv-2024-zf1m7.
- [35] M. P. Sowiński, A.-L. Warnke, B. A. Lund, S. Skagseth, D. B. Cordes, J. E. Lovett, M. M. Haugland, *Replication Data for: Spirocyclic pyrrolidinylnitroxides with exo-methylene substituents, DataverseNO, V1* **2024**, DOI: 10.18710/PIZ7H1.

Manuscript received: June 3, 2024
Revised manuscript received: July 29, 2024
Accepted manuscript online: July 29, 2024
Version of record online: September 17, 2024